Special Issue – TANGO

International journal of spray and combustion dynamics

International Journal of Spray and Combustion Dynamics
0(0) 1–11

DOI: 10.1177/1756827718782884
journals.sagepub.com/home/scd

SAGE

Intrinsic thermoacoustic modes and their interplay with acoustic modes in a Rijke burner

N Hosseini[1,2], VN Kornilov[1], I Lopez Arteaga[1,3], W Polifke[4], OJ Teerling[2] and LPH de Goey[1]

Abstract

The interplays between acoustic and intrinsic modes in a model of a Rijke burner are revealed and their influence on the prediction of thermoacoustic instabilities is demonstrated. To this end, the system is examined for a range of time delays, temperature ratios and reflection coefficients as adjustable parameters. A linear acoustic network model is used and all modes with frequency below the cut-on frequency for non-planar acoustic waves are considered. The results show that when reflection coefficients are reduced, the presence of a pure ITA mode limits the reduction in the growth rate that usually results from a reduction of the reflection coefficients. In certain conditions, the growth rates can even increase by decreasing reflections. As the time delay of the flame and thus the ITA frequency decreases, the acoustic modes couple to and subsequently decouple from the pure ITA modes. These effects cause the maximum growth rate to alternate between the modes. This investigation draws a broad picture of acoustic and intrinsic modes, which is crucial to accurate prediction and interpretation of thermoacoustic instabilities.

Keywords

Intrinsic thermoacoustic instability, Rijke burner, network model, acoustic mode, ITA mode

Date received: 19 May 2017; accepted: 30 April 2018

1. Introduction

Thermoacoustic instabilities constitute a major branch of combustion instabilities that are undesirable for combustion systems designed to work steadily. Such instabilities are a result of a strong coupling between the system acoustics and fluctuating heat generation. The acoustic fluctuations modulate the heat release and this in turn produces acoustic waves. A thermoacoustically unstable system may exhibit pressure fluctuations with an amplitude in the order of audible sound (in e.g. heating appliances) up to operating pressure levels (in e.g. rocket engines). These pressure fluctuations limit the operating range of the system or even cause structural damage and thus should be avoided or controlled.

The common practice in studying thermoacoustic instabilities is to first identify the coupling between the active elements (such as burners and heaters) and the acoustic field. Then it is possible to calculate the complex eigenfrequencies of the system including the active and passive elements (such as ducts, area changes and terminations). This approach is used in the framework of the so-called network models and numerical Helmholtz solvers. In traditional thermoacoustics, it is understood that for a system to be thermoacoustically unstable, a coupling should exist between the active elements and the acoustic reflections from the rest of the system. However, it was established recently that a

[1]Mechanical Engineering Department, Eindhoven University of Technology, Eindhoven, the Netherlands
[2]Bekaert Combustion Technology BV, Assen, the Netherlands
[3]Department of Aeronautical and Vehicle Engineering, KTH Royal Institute of Technology, Stockholm, Sweden
[4]Mechanical Engineering Department, Technische Universität München, Garching, Germany

Corresponding author:
N Hosseini, Mechanical Engineering Department, Eindhoven University of Technology, P.O. Box 513, 5600 MB Eindhoven, the Netherlands.
Email: naseh.hosseini@gmail.com

combustor may be unstable even in the absence of any acoustical reflections upstream or downstream of the burner. In practice, such conditions have been observed as instabilities that do not respond adequately to the changes in upstream and/or downstream acoustic properties.[1] This type of instabilities is thought to originate from an inherent coupling within the burner itself and are called intrinsic thermoacoustic (ITA) instabilities.

The modes of the coupled acoustic-flame system tend to be associated either to an ''acoustic mode'' or to an ''ITA mode'', with the acoustic modes being associated to cavity acoustic oscillations and the ITA modes being associated to the inherent coupling of the burner. In addition, the system modes can be evaluated in two limit cases that help investigating their properties. The first case is when all elements in the system are considered thermoacoustically passive, and the obtained modes are called ''pure acoustic modes''. The other case is when the system boundaries or the boundaries at the interfaces of a selected element are considered non-reflecting, and the obtained modes are called ''pure ITA modes''.

Bomberg et al.[2] have shown that when the flame scattering matrix is represented with respect to causality, a pole of the transfer matrix can be found at a specific frequency. The gains of the scattering matrix elements are maximum at this frequency, showing that some kind of resonance is expected. They used experimentally measured transfer functions (TFs) of a stable and an unstable burner to demonstrate the difference in the thermal and acoustic responses of the flames. They identified the ITA feedback loop through the acoustics-flow-flame-acoustics coupling and were able to relate the experimentally observed instability to the ITA instability. Hoeijmakers et al.[3] theoretically showed that the transfer matrix poles correspond to the frequencies at which the phase of the flame/burner TF crosses odd multiples of π. This means that, theoretically, any active acoustic element that has a TF phase of at least π, has at least one ITA mode. They also performed measurements with nearly anechoic conditions upstream of the burner and showed that the trends of the observed instabilities are as can be expected from tracking the poles of the transfer matrix. Therefore, they concluded that the observed instability was an ITA mode. These two studies initiated a series of additional studies on the ITA instabilities in the past few years. Emmert et al.[4] used a simplified network model, and Courtine et al.[5] and Silva et al.[6] used DNS to confirm and capture ITA instabilities in confined laminar premixed Bunsen flames.

The initial investigations on ITA instabilities have created the motivation and momentum for the community to investigate ITA instabilities in more detail. Consequently, recent studies have focused on studying their behavior. Hoeijmakers et al.[7] have numerically shown that in practice a mode of the coupled acoustic-flame system (where reflections are not perfect) could be a combination of pure acoustic and ITA modes. In addition, Silva et al.[8] recently reported measurements showing acoustic modes and ITA modes occurring simultaneously in a swirl combustor. In order to make adequate mitigating choices it is very important to identify if an unstable mode is acoustic or ITA. In a recent study, Emmert et al.[9] used experimentally measured values of flame TF within a network model and introduced a matrix transformation method that allowed them to decouple acoustic and ITA modes from full system modes. By performing a sweep on a defined coupling parameter, they observed that some system modes originate from pure acoustic and others from pure ITA modes. Their procedure identifies the ITA modes, but the coupling parameter does not have a physical representation and reducing it to values below unity is unphysical. Albayrak et al.[10] have very recently introduced a convective scaling for ITA modes of a premixed swirl combustor. They have shown that including flow inertia affects the frequencies of ITA modes and the frequencies found using the modified approach better match with the experimentally observed unstable frequencies. These effects are significant in burners with large flow inertia, thus area change. Their new criterion helps in associating the peaks observed in the sound pressure level spectra to either ITA or acoustic modes.

In a general scheme, the peculiarity of the problem we consider is that an element with internal feedback is placed inside a system with external feedback, and then some interplay between these two feedback loops may be expected. This situation is generic and may be encountered in different branches of science. One physically close situation was studied in another branch of acoustic research, which also may be interpreted in terms of intrinsic and external feedback interplay. The example is the edge-tone configuration, which consists of a planar jet from a thin slit that interacts with a thin sharp edge placed parallel to the slit further downstream. The jet oscillations observed in this configuration are essentially a hydrodynamic instability.[11] Moreover, it is well known that acoustical feedback from surroundings influences the oscillation frequency and amplitude. Some experiments have shown that the oscillation frequency of an edge-tone placed above a table was affected by the reflection of acoustic waves from the table.[11] It was also observed that surrounding geometries affect the unstable frequency of the system. When the system is placed in the opening of a pipe, the edge-tone becomes an organ pipe and forms strong acoustical feedback. In such configurations, the edge-tone is not dominant; however, it plays a significant

role in the transients of the flue instruments.[12,13] Additionally, Castellengo[14] has shown that the edge-tone modes depend strongly on the geometry of the mouth of the instrument. While for a recorder (where the jet length W is typically four times the jet thickness h) only one edge-tone mode is active, for typical organ pipes (where W/h can be as large as 12 or 20) many edge-tone modes are observed. Therefore the attack transient of an organ-pipe is often much more complex than that of a recorder.

Most of the research on ITA instabilities has been focused on establishing a fundamental base for confirming the existence and importance of ITA instabilities. In addition, using available experimental data to confirm the findings has narrowed the window of investigation to specific case studies. However, a broader picture of ITA and acoustic modes in a system is required in order to unveil more of the independent and coupled behavior of these modes. In addition, it is not always obvious whether a given mode is acoustic or ITA, and whether any interplay exists between these modes.

This work aims to address these issues by identifying ITA modes using multiple parametric sweeps. A Rijke burner (a combustor with a flame and temperature change, but no area change) is investigated using a linear acoustic network model. All the system modes with frequency below the cut-on frequency for non-planar acoustic waves are studied. This frequency range is usually below 1 kHz which is the range of focus for most thermoacoustic instability studies. The system is examined for a range of values of flame time delays, temperature ratios and reflection coefficients. Therefore, this work provides a parametric study that governs a wide range of parameters; however, not every combination of parameters is likely to have some corresponding realistic configuration. Nevertheless, these parameters and their corresponding values are chosen based on (but not limited to) the realistic conditions where thermoacoustic instabilities may occur.

The time delay and temperature ratio are directly related to the combustion properties of the burner. A leaner flame results in larger time delays and smaller temperature ratios. In addition, the use of non-conventional fuels can also result in various combinations of flame time delays and temperature ratios.[15] Moreover, a constant temperature ratio and varying time delay can mimic the cold start for perforated premixed burners, since the stabilization temperature has a large impact on the flame time delay.[1] On the other hand, the actual acoustic conditions at the boundaries are not ideal, due to the presence of other parts, and the reflection coefficients can vary. In addition, changing the downstream temperature is meant to reveal the effects of the shift in resonance frequencies and reducing the reflection coefficients towards zero to include the limits of anechoic environment. Therefore, the four mentioned parameters are chosen for the parametric studies.

The results show complicated, yet interesting, interplays between the acoustic and ITA modes in the system. They reveal how an acoustic mode is affected by a pure ITA mode and how these effects create large growth rates in multiple system modes. The movie submitted as supplementary material very well visualizes these effects and interplays. This investigation draws a larger picture of ITA instabilities and demonstrates that such parametric investigations on multiple system modes are crucial to obtaining correct predictions and interpretations of the instabilities in the system.

2. Theory of ITA instabilities

The approach in this article follows the one described in the work of Emmert et al.[16] The pressure fluctuations (p') and velocity fluctuations (u') together with the Riemann invariants f and g, are used to describe the propagation of acoustic waves. The upstream (u) and downstream (d) waves for the flame are illustrated in Figure 1, where $u' = f\text{-}g$ and $p'/\rho c = f+g$.

For an acoustically compact flame (when its length is negligible compared to the acoustic wavelength) the Rankine-Hugoniot jump conditions[17] can be applied and the scattering matrix can be obtained. In low Mach number flows the upstream and downstream pressure and velocity perturbations are related as

$$\begin{bmatrix} \frac{p'_d}{\rho_d c_c} \\ u'_d \end{bmatrix} = \begin{bmatrix} \varepsilon & 0 \\ 0 & 1 \end{bmatrix} \begin{bmatrix} \frac{p'_u}{\rho_u c_u} \\ u'_u \end{bmatrix} + \begin{bmatrix} 0 \\ \theta TF u'_u \end{bmatrix} \quad (1)$$

where TF is a velocity-sensitive transfer function as $q'/q = TF(u'/u)$ to describe the relation between velocity fluctuations (u') and heat release fluctuations (q'). $\theta = (T_d/T_u) - 1$ denotes the dimensionless temperature ratio and $\varepsilon = (\rho_u c_u)/(\rho_d c_d)$ denotes the ratio of specific impedances. These two ratios can be related based on some assumptions. Since thermoacoustic instabilities usually occur in lean combustion of light hydrocarbons, such as methane, the number of moles remains almost constant in the reactions, so the average molecular

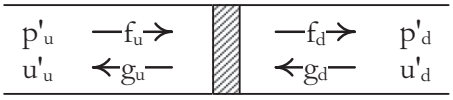

Figure 1. The upstream (u) and downstream (d) waves for the flame.

weight does not considerably change. If the mixture is also assumed a perfect gas then $\theta=\varepsilon^2-1$ relates the dimensionless temperature ratio to the ratio of specific impedances.[2,15]

The feedback loop is well described by Bomberg et al.[2] and Albayrak et al.[10] and shows that the intrinsic feedback does not involve the acoustic reflections at the combustor inlet and/or outlet. It is illustrated in Figure 2 with red colors showing that the upstream travelling wave (c_2) generated by flame heat release, influences the velocity fluctuations upstream of the burner.

Respecting causality in defining the input and output waves leads to the scattering matrix as

$$\begin{bmatrix} f_d \\ g_u \end{bmatrix} = SM \begin{bmatrix} f_u \\ g_d \end{bmatrix} \tag{2}$$

and using straightforward linear algebra we can obtain

$$SM = \frac{1}{1+TF(\varepsilon-1)} \begin{bmatrix} \dfrac{2\varepsilon(1+\theta TF)}{\varepsilon+1} & -\dfrac{1+\theta TF-\varepsilon}{\varepsilon+1} \\ \dfrac{1+\theta TF-\varepsilon}{\varepsilon+1} & \dfrac{2}{\varepsilon+1} \end{bmatrix} \tag{3}$$

The poles of the scattering matrix are obtained when the denominator in equation (3) equals zero, i.e. when $TF(\varepsilon-1)=-1$. These poles correspond to the pure ITA modes of the system.[2,7] Since ε is real, this is only satisfied when TF is also real. Therefore, the TF phase φ of pure ITA frequencies should equal odd multiples of π and gain is $1/(\varepsilon-1)$.

In order to close the coupling between the heat release and velocity fluctuations, the n-τ model is used. This model is a "velocity-coupled" flame response model and assumes that the unsteady heat release is proportional to the unsteady flow velocity, multiplied by the interaction index n, and delayed in time by the time delay τ.[18] Therefore we have, $TF=ne^{i\omega\tau}$. The value of the time delay determines the change of TF phase with frequency. It is important to note that n shows the ratio of the magnitude of the "fluctuations" of the heat release to velocity, while θ shows the "mean" change of temperature, and thus, velocity. An acoustically passive flame has a zero n, but can have a nonzero θ. More detailed discussion of the role and definition of the passive/active properties of the elements of a network in application to the thermoacoustic instability analysis can be found in the work of Kornilov et al.[19]

If the time delay is assumed frequency-independent, the following expression can be realized for the pure ITA mode of order m

$$2\pi f_m = \frac{\varphi_m}{\tau} = \frac{(2m-1)\pi}{\tau} \Rightarrow f_m = \frac{2m-1}{2\tau}, \qquad m=1,2,\ldots, \tag{4}$$

where f_m and φ_m are the frequency and TF phase, respectively. Defining the Strouhal number as the non-dimensional frequency, we have

$$St = f_m\tau = m-0.5, \qquad m=1,2,\ldots, \tag{5}$$

The next section contains the description of the Rijke burner setup and its corresponding acoustic network model, which is chosen to investigate the behavior of the acoustic and ITA modes.

3. The Rijke burner and its equivalent acoustic network model

An illustration of the Rijke burner showing the dimensions, location of the flame, upstream and downstream temperatures, and assumed flow direction is presented in Figure 3. In this study, the flow is not modeled since its Mach number is small and its acoustic effects are negligible. In addition, the flame is compact and its thickness is negligible in comparison with the tube length.

Figure 4 contains the equivalent acoustic network model of the Rijke burner. Here the only active element is the flame and the rest of the system are passive elements (ducts and terminations).

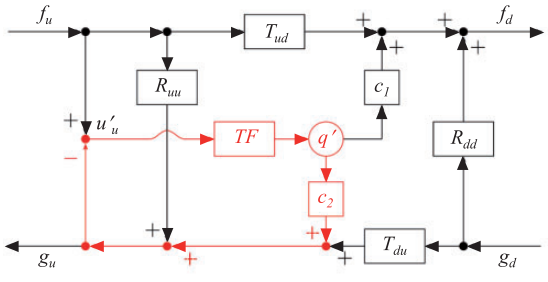

Figure 2. The internal intrinsic feedback loop in a combustor. R and T denote the reflection and transmission coefficients upstream and downstream of the burner (recreated from Albayrak et al.[10]).

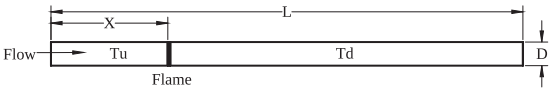

Figure 3. The Rijke burner model showing the combustor length L, diameter D, flame location X, upstream temperature T_u, downstream temperature T_d and assumed flow direction.

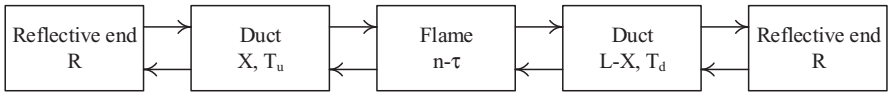

Figure 4. The equivalent acoustic network model of the Rijke burner.

The dimensions and values used in the current investigation are summarized as $L=1\,\text{m}$, $X=0.25\,\text{m}$, $T_u=300\,\text{K}$, $T_d\in[450{:}150{:}1800]\text{K}$, $\theta\in[0.5{:}0.5{:}5]$, $n=1$, $\tau\in[0{:}0.1{:}5]\text{ms}$ and $R\in[-1{:}0.2{:}0]$. The tube diameter D needs to be small enough (in comparison with a cut-off diameter of the lowest frequency of propagation of transversal modes) to limit the system to only one-dimensional propagation of longitudinal acoustic waves. The fluid is considered air with temperature-dependent density and speed of sound. The flame time delay τ covers a large range of values encountered in academic cases, such as heated wires and laboratory Bunsen flames, as well as practical combustion systems, such as gas turbines and heating appliances. The dimensionless temperature ratio θ is calculated as $\theta=(T_d/T_u)-1$. Finally, the reflection coefficients at the upstream and downstream ends are varied from -1 (fully reflecting open end) to 0 (non-reflecting), and are assumed equal, real and frequency-independent.

The constructed model is solved using taX,[16] a state-space network modelling tool developed by Technical University of Munich. This network model is a low order simulation tool for the propagation of acoustic waves in acoustic network systems and is able to determine the stability, mode shapes, frequency responses, scattering matrices and stability potentiality of the acoustic networks of arbitrary topology. The parametric studies create 3060 cases, for which all the system modes within the frequency range of interest are investigated. This broad investigation is expected to reveal details of the behavior of the acoustic and ITA modes as well as their possible interplays. In the following sections, the results are presented predominantly in the form of pole-zero plots showing the eigenfrequencies and the corresponding growth rates of the system modes.

4. Results and discussion

The figures presented in this section show all the system modes in the frequency window of interest. The complete sweep on time delay is performed with steps of 0.1 ms. However, the data are presented only for a few selected values, i.e. with steps of 0.5 ms. For the complete version and better impression of the trends, the reader is encouraged to see the video file submitted as supplementary material, because the high resolution animation shows the "motion" of the modes. Each frame of the animation shows the data for a specific time delay. Therefore, using the Strouhal number would mean to multiply the frequency data by the value of time delay in every frame. In addition, the Strouhal number changes as the time delay increases and this makes interpretation of the graphs more complicated. This is why the data are presented in terms of absolute frequency for this set of graphs. The center of each circle shows the frequency and growth rate of a system mode, and the radius scales with respect to the temperature ratio. The colors show the change in the reflection coefficients according to the included color map. Therefore, the black circles represent the pure ITA modes of the system. In the next two subsections, the results are split in groups of small ($\tau<1\,\text{ms}$) and large ($\tau\geq1\,\text{ms}$) time delays. The reference for this categorization is the practical range encountered in academic and industrial burners. Since the time delay is related to the convective time of perturbations in the flame, small flames usually have smaller time delays than large ones. The time delay of small laminar premixed perforated burners is usually below 2 ms, but for large turbulent swirl flames in gas turbines, it can be as large as 7 ms.

4.1 Small time delays ($0\leq\tau<1$ ms)

The data for $\tau=0$, 0.5 and 0.8 ms are presented in Figure 5. When $\tau=0$ ms (Figure 5(a)), no instability is expected and all system modes are stable, i.e. the growth rate is negative. Here, decreasing the reflection coefficients (increasing acoustic losses) only further stabilizes the system modes. This is the well-known behavior of acoustic modes. In addition, it is easy to distinguish the first, second and third modes of the system around the frequencies of 250, 550 and 900 Hz, respectively, along with the fourth mode for the cases with small temperature ratios around the same frequencies as the third mode (the sweep on the temperature ratio causes overlaps in the frequency ranges of some modes). By increasing τ from 0 to 0.5 ms, the first and third mode start to destabilize, while the second mode further stabilizes. This result is expected based on the location of the flame and has been observed experimentally as well.[20] However, as τ approaches 0.5 ms (see the supplementary video file), the growth rate of the third mode increases to one order of magnitude larger than that of the first mode. When $\tau=0.5\,\text{ms}$, the first pure ITA mode enters the window of investigation and it is revealed that the third mode is significantly affected by the proximity of this

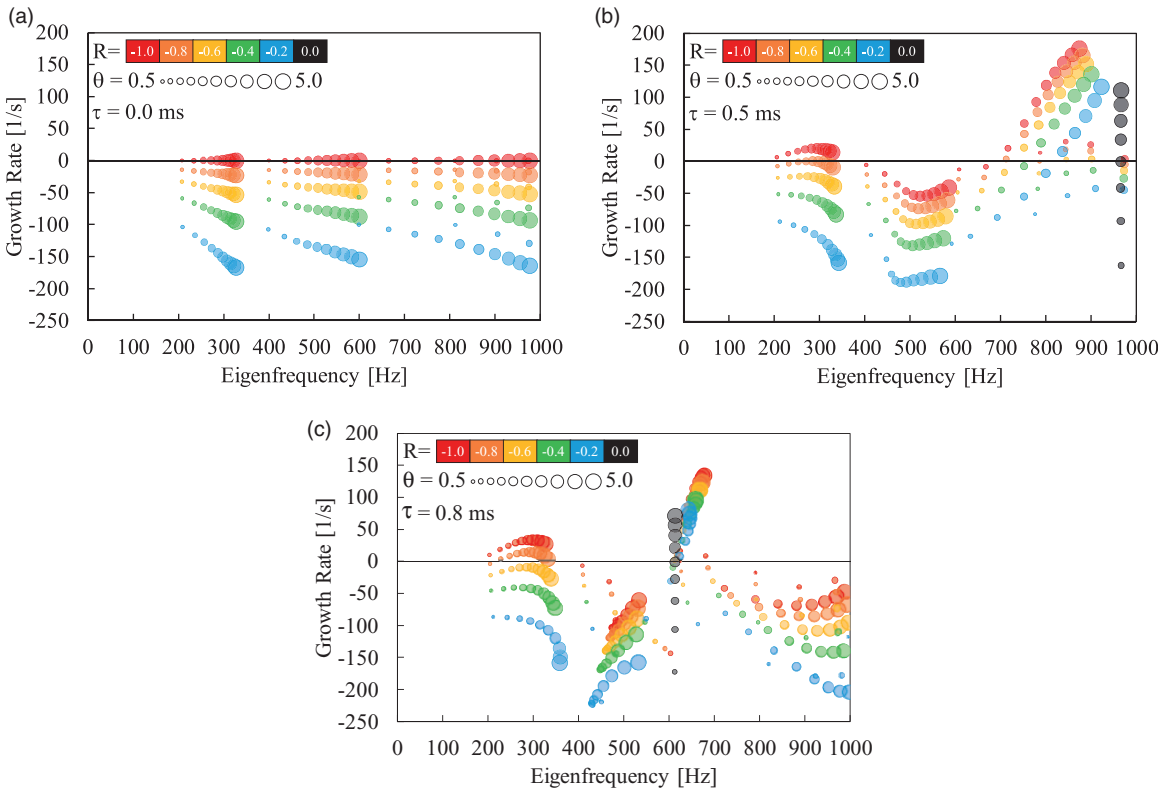

Figure 5. The eigenfrequencies and growth rates of all system modes when $\tau = 0$ (a), 0.5 (b) and 0.8 ms (c), $\theta \in [0.5{:}0.5{:}5]$ (scaled by marker size) and $R \in [-1{:}0.2{:}0]$ (scaled by color).

pure ITA mode. Therefore, the third mode which was an acoustic mode for smaller values of τ is now an ITA mode. Therefore, the system now has two acoustic and one ITA modes in the investigated frequency range. By slightly increasing the time delay to $\tau = 0.8$ ms (Figure 5(c)), a new acoustic mode enters the window of investigation following the first pure ITA mode, so that the system always has its three acoustic modes. This reconfirms the conclusions of Emmert et al.[9] about the total number of system modes being equal to the summation of acoustic and pure ITA modes.

In addition, decreasing reflection coefficients when $\tau = 0.5$ ms makes the first and second mode more stable, while the third mode converges to the first pure ITA mode, which is unstable for $\theta > 3$. In practice, this means that in a Rijke burner that has a flame with a small time delay, increasing the mean heat release (by using higher powers for example) can shift the instability from the first to the third mode. This depends also on the damping of these modes and the frequency dependence of the reflection coefficient, which in turn increases with combustor diameter. Nevertheless, similar effects have been observed experimentally before, but are not taken into account in this study.

In order to take a closer look at the "convergence" of system modes to pure ITA modes, a finer sweep is performed on the reflection coefficients between −0.2 and 0. The results for the third mode are plotted in Figure 6. Here it can be seen in more detail that the continuous convergence to pure ITA modes occurs only when $\theta \geq 3.5$. It is important not to mistake this limit with the critical gain criterion in pure ITA modes. This criterion includes a critical value of the gain of the flame TF, above which the growth rate of the pure ITA mode is positive. It has been derived analytically in previous works.[4,5,7] For the investigated

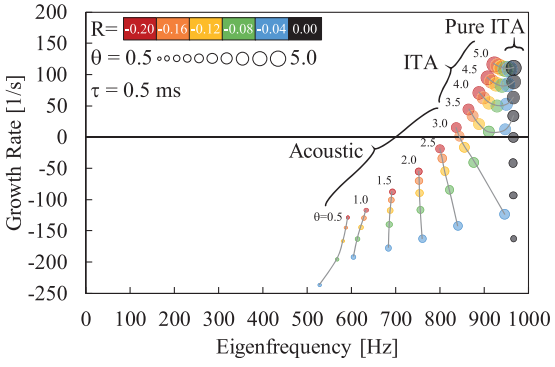

Figure 6. The eigenfrequencies and growth rates of all system modes when $\tau = 0.5$ ms, $\theta \in [0.5{:}0.5{:}5]$ (scaled by marker size) and $R \in [-0.2{:}0.04{:}0]$ (scaled by color).

configuration, the critical gain of $n=1$ occurs at $\theta=3$, which is in agreement with the theory.[5]

If the system is operating in $\theta \geq 3.5$ conditions, increasing acoustic losses does not fully stabilize the system. These modes are known as ITA modes.[9] In addition, Figure 6 demonstrates that as the reflections decrease, the growth rates of the ITA modes can change non-monotonically (follow the line of reducing reflections for $\theta=3.5$). It can also be deduced that in the presence of very small reflections, increasing θ from 3 to 3.5 dramatically changes the growth rate and a splitting occurs in the trend due to the presence of a pure ITA mode close to this frequency.

4.2 Large time delays ($\tau \geq 1$ ms)

The eigenfrequencies and growth rates of all system modes for $\tau=1$ and 1.5 ms are plotted in Figure 7. As the time delay increases to 1 ms (Figure 7(a)), the frequency of the first pure ITA mode reduces to around 500 Hz and the distribution of the system modes becomes more complicated. As the pure ITA mode moves to lower frequencies, it "drags" the ITA mode with it and pushes the neighboring acoustic mode (the second mode) towards lower frequencies. In Figure 7(a), it is visible that the third mode now has a frequency around 600 Hz, while it was around 800 Hz for $\tau \leq 0.5$ ms, and it is still an ITA mode (i.e. it converges to the first pure ITA mode as the reflections decrease). On the contrary, other modes are acoustic modes and stabilize as the reflections decrease.

When $\tau=1.5$ ms (Figure 7(b)), the third mode is switched back to an acoustic mode and the first pure ITA mode is now affecting the first mode. Here, a "movement" convention is chosen to describe these interplays (the reader is encouraged to follow this process with the supplementary video file). As a pure ITA mode passes an acoustic mode, it attaches to the acoustic mode, turning it into an ITA mode (if the temperature ratio is large enough), and then drags it along towards lower frequencies. The pure ITA mode eventually detaches from the ITA mode (causing it to become acoustic again) only to immediately attach to another lower acoustic mode. This "attachment" and "detachment" occur around the frequency of the third (900 Hz) and second (500 Hz) pure acoustic modes, respectively. This occurs in such a way that the total number of modes is equal to the summation of the number of pure acoustic and pure ITA modes. This has been observed for a specific set of system parameters in a previous study,[9] but here it is shown that it holds for almost any combination of the governing parameters.

When $\tau=1.5$ ms (Figure 7(b)), the second pure ITA mode has the frequency of about 1 kHz and creates the same effect as the first pure ITA mode when the time delay was 0.5 ms (Figure 5(b)). This behavior repeats as new pure ITA modes enter the window of investigation and is very well illustrated in the supplementary video file and Figure 8. It is obvious that increasing the time delay results in more and more pure ITA modes to enter the window of investigation. However, it can be observed that new acoustic modes also enter the window of investigation, following the pure ITA modes. The interplay between the acoustic and pure ITA modes of the system is complicated, but repetitive. The pure ITA mode holds to the system ITA mode if there are no lower acoustic modes to which it can attach. Therefore, they remain stitched together as a pack of ITA modes. This is visible for the first mode in Figure 8.

The results are so far presented in the form of snapshots of the supplementary video file at specific time delays which includes the whole parameter range. In order to better study how acoustic modes are affected by pure ITA modes, it is efficient to choose a specific temperature ratio and reflection coefficient and investigate the trends in more detail. This analysis is presented in the next section.

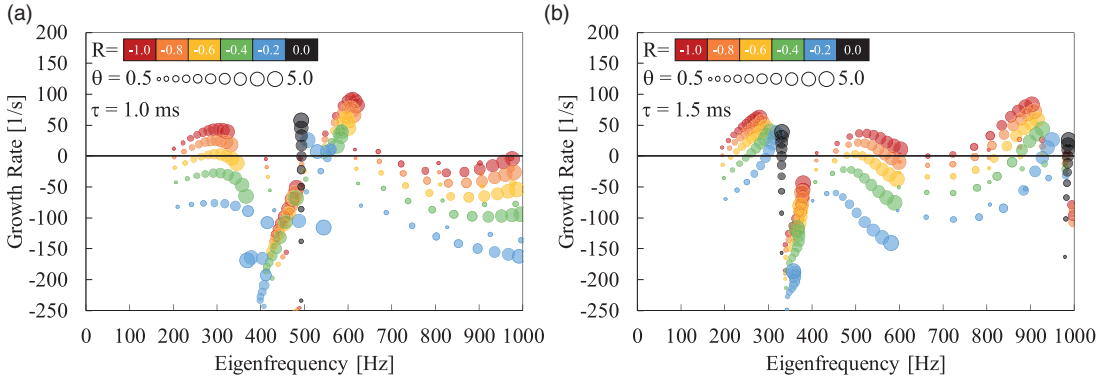

Figure 7. The eigenfrequencies and growth rates of all system modes when $\tau=1$ (a) and 1.5 ms (b), $\theta \in$[0.5:0.5:5] (scaled by marker size) and $R \in$[−1:0.2:0] (scaled by color).

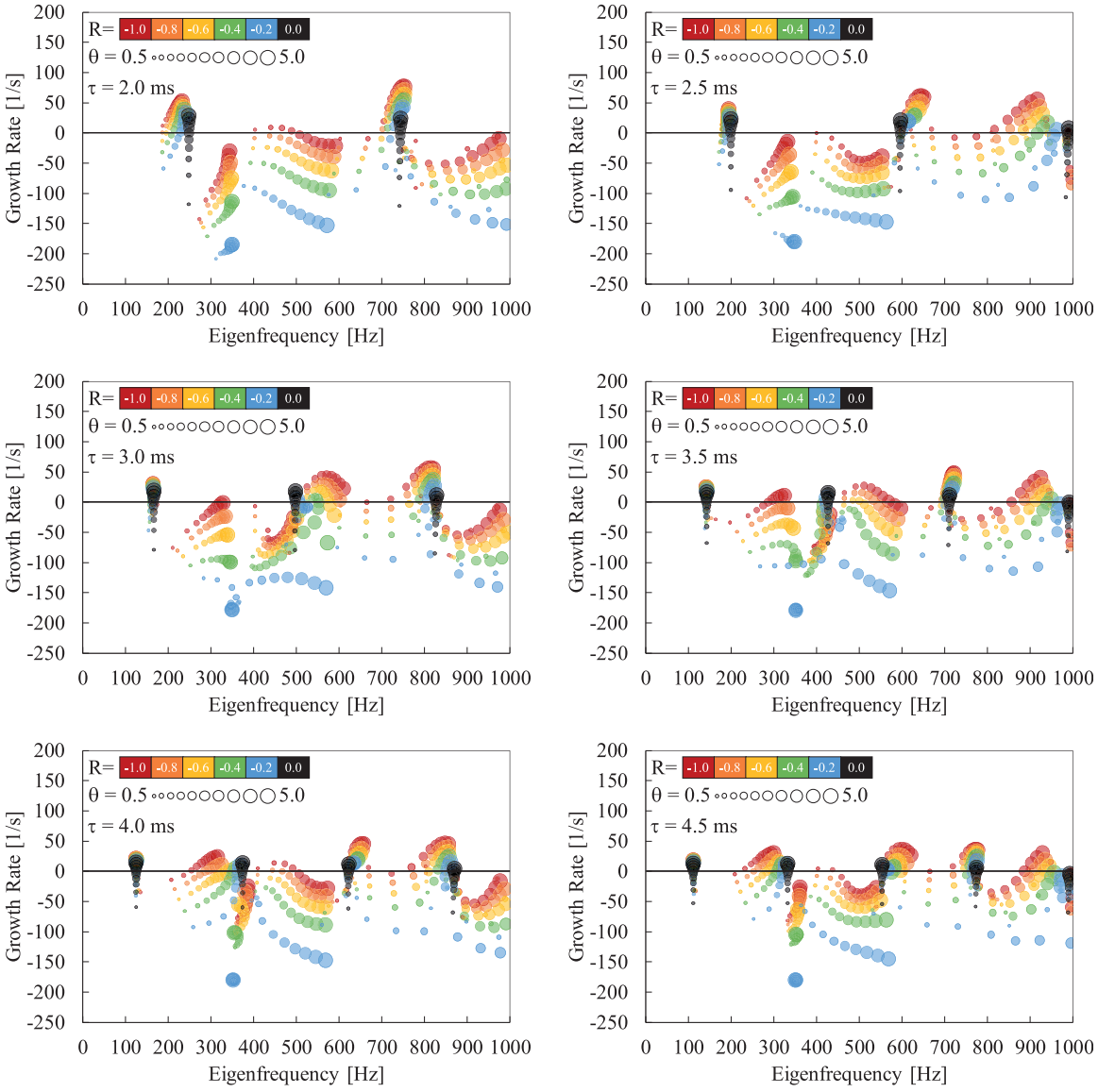

Figure 8. The eigenfrequencies and growth rates of all system modes when $\tau \in [2{:}0.5{:}4.5]$ ms, $\theta \in [0.5{:}0.5{:}5]$ (scaled by marker size) and $R \in [-1{:}0.2{:}0]$ (scaled by color).

4.3 The behavior of system modes near pure ITA modes

Here, the temperature ratio $\theta = 5$ and reflection coefficient $R = -1$ are chosen and the system modes are evaluated in terms of growth rate and Strouhal number $St = f\tau$. These values correspond to combustors with large temperature ratio and open inlet and outlet. Usually, high growth rates are expected for these conditions, which are expected based on the absence of acoustic energy losses at the boundaries and the contribution of the temperature ratio to the acoustic energy gain. In addition, the time delay is further increased to 10 ms in order to evaluate the system behavior for large Strouhal numbers.

Figure 9 illustrates how the Strouhal numbers of the first six system modes change with the time delay. The fixed Strouhal numbers of the pure ITA modes are illustrated with horizontal dotted lines with their values corresponding to equation (5), and the convergence of the first, second, and third system modes to their corresponding pure ITA modes is visible. If no pure ITA modes were present, one could expect that the Strouhal number uniformly increases with time delay. However, this figure clearly illustrates the attaching and detaching of the acoustic modes to pure ITA modes in the form of limiting the increase of Strouhal number with time delay when the Strouhal number of the mode is close to that of a pure ITA mode. This effect is less significant for higher modes and lower

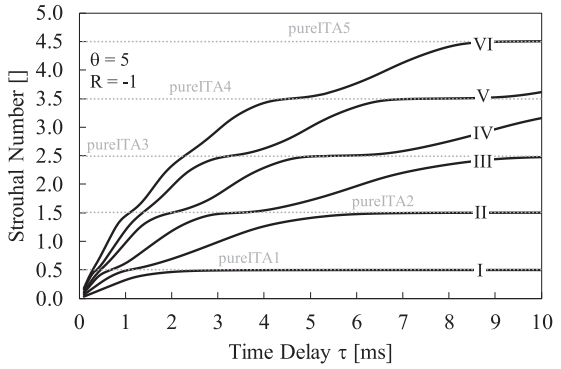

Figure 9. Changes in the Strouhal number of the first six system modes with time delay. The mode number is shown in Latin numbers, $\theta = 5$ and $R = -1$.

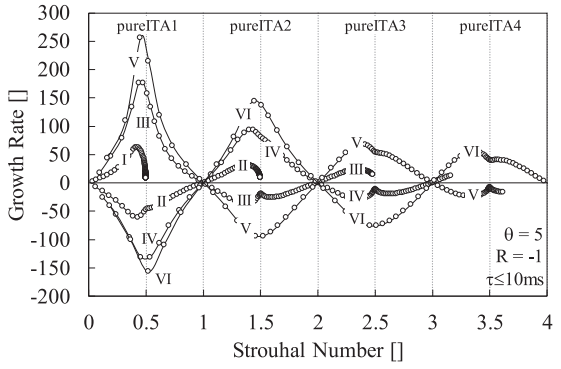

Figure 10. The first six system modes (indicated with Latin numbers) when $\theta = 5$, $R = -1$ and $\tau \in [0{:}0.1{:}10]$ ms (each marker indicates a system mode for a specific value of τ).

pure ITA modes, but increases for higher pure ITA modes.

The slope of the curve corresponding to a specific system mode in Figure 9 may be used as a criterion to define whether the mode is acoustic or ITA. One may define the system mode ITA, i.e. the mode is affected by the presence of the pure ITA mode, when this slope is smaller than a certain value (it is zero for pure ITA modes).

The complete picture of the mode behavior is obtained when the growth rates are also included. Figure 10 illustrates the Strouhal numbers and growth rates of the first six system modes (indicated with Latin numbers) for the investigated range of parameters (each marker indicates a system mode). Distinct fluctuations between stability and instability are visible for all the modes and these fluctuations have a counter behavior for the even and uneven modes. This behavior is expected based on the combination of τ and the location of the heat source. These fluctuations are also visible in the animated video file submitted as supplementary material. The maxima and minima occur very close to the Strouhal number of the pure ITA modes; however, they deviate from it as the Strouhal number increases. Moreover, all system modes have zero growth rate for integer Strouhal numbers.

In addition, Figure 10 shows that higher order modes have, in general, larger growth rates and their maximum growth rate decreases as Strouhal number increases. If the growth rates of these modes are large enough, they may overcome their acoustic damping and take over the system instability from the usual first-mode instability in a Rijke burner. Therefore, it is important to investigate higher order modes to be able to see such differences.

Investigating the system modes for various ranges of parameters provides a large picture of the system modes and reveals the complex interplay between the acoustic and intrinsic modes. Although the investigation is performed on a Rijke burner, the revealed interplays are expected to be similar in more practical configurations when only longitudinal acoustic modes are considered. Therefore, the conclusions drawn in the next section are generic in nature and can be extended to other particular cases.

5. Conclusions

The thermoacoustic instabilities in a Rijke burner are investigated focusing on the ITA modes and their interplay with the acoustic modes. A linear network model is used and multiple parametric studies are performed with varying values of time delay, temperature ratio, and reflection coefficients, covering a broad range corresponding to various (sometimes extreme) operating conditions of a combustor. This parametric study mimics practical situations, such as cold start (almost constant temperature and varying time delay) and changes in fuel composition (slowly varying temperature ratio and quickly varying time delay).

The results show that the pure ITA and acoustic modes constantly interplay with each other, even for small values of flame time delay. While the common belief for ITA modes to be effective is that the time delay needs to be relatively large, this investigation shows that ITA modes may be specifically responsible for the highest growth rates when time delay is relatively small (around 0.5 ms). In addition, the maximum growth rate occurs in different modes for different values of time delay. Therefore, the complete effects of ITA instabilities are better captured if the investigation is not limited to specific values of time delay or the first acoustic mode.

When reflection coefficients are reduced, the presence of a pure ITA mode near an acoustic mode limits the

reduction in the growth rate of the mode to that of the pure ITA mode. In certain conditions, the growth rate of this mode increases by decreasing reflections. This means that a system that has an unstable ITA mode might become even more unstable if acoustic damping is introduced at the reflective ends. Therefore, defining the characteristics of the instability by multiple parametric studies is useful before an abatement method is selected.

As the time delay increases, the number of pure ITA modes also increases and creates complicated mode overlapping. However, the observed behavior of the system modes with increasing time delay is periodic in nature, i.e. system modes couple to and subsequently decouple from pure ITA modes and become stable and unstable. This phenomenon is also seen in the form of an ITA mode attaching to a pure ITA mode for certain time delays, and then detaching from it and becoming an acoustic mode again. This motivates finer parametric investigations when thermoacoustic instabilities are investigated in a real setup in order to identify the details of the occurred mode. In addition, this observation may be a potential cause of mode switching in situations with varying time delay, such as cold start.

In this investigation, interplays are revealed between the acoustic and intrinsic modes in the system. The behaviors of these interplays are studied and it is demonstrated that for a correct prediction of thermoacoustic instabilities, it is crucial to create a broad picture of system behavior showing how various system modes react to the changes of effective parameters. Moreover, the observed effects have similarities with other systems in other branches of physics that motivates a future multidisciplinary holistic study on the systems with internal and external feedback in order to reveal the common underlying mathematics.

Acknowledgements

The presented work is part of the Marie Curie Initial Training Network, Thermo-acoustic and aero-acoustic nonlinearities in green combustors with orifice structures (TANGO).

Declaration of Conflicting Interests

The author(s) declared no potential conflicts of interest with respect to the research, authorship, and/or publication of this article.

Funding

The author(s) disclosed receipt of the following financial support for the research, authorship, and/or publication of this article: European Commission under call FP7-PEOPLE-ITN-2012.

ORCID iD

N Hosseini http://orcid.org/0000-0003-0998-4977.

Supplement Material

Supplement material for this article is available online at https://youtu.be/2lIcAViB3mM

References

1. Poinsot T. Prediction and control of combustion instabilities in real engines. *Proc Combust Inst* 2017; 36: 1–28.
2. Bomberg S, Emmert T and Polifke W. Thermal versus acoustic response of velocity sensitive premixed flames. *Proc Combust Inst* 2015; 35: 3185–3192.
3. Hoeijmakers PGM, Lopez Arteaga I, Kornilov V, et al. Experimental investigation of intrinsic flame stability. In: *Proceedings of the European combustion meeting*, Lund University, Sweden, 25–28 June 2013.
4. Emmert T, Bomberg S and Polifke W. Intrinsic thermoacoustic instability of premixed flames. *Combust Flame* 2015; 162: 75–85.
5. Courtine E, Selle L and Poinsot T. DNS of intrinsic thermoacoustic modes in laminar premixed flames. *Combust Flame* 2015; 162: 1–11.
6. Silva CF, Emmert T, Jaensch S, et al. Numerical study on intrinsic thermoacoustic instability of a laminar premixed flame. *Combust Flame* 2015; 162: 3370–3378.
7. Hoeijmakers PGM, Kornilov V, Lopez Arteaga I, et al. Intrinsic instability of flame-acoustic coupling. *Combust Flame* 2014; 161: 2860–2867.
8. Silva CF, Merk M, Komarek T, et al. The contribution of intrinsic thermoacoustic feedback to combustion noise and resonances of a confined turbulent premixed flame. *Combust Flame* 2017; 182: 269–278.
9. Emmert T, Bomberg S, Jaensch S, et al. Acoustic and intrinsic thermoacoustic modes of a premixed combustor. *Proc Combust Inst* 2017; 36: 3835–3842.
10. Albayrak A, Steinbacher T, Komarek T, et al. Convective scaling of intrinsic thermo-acoustic eigenfrequencies of a premixed swirl combustor. *ASME J Eng Gas Turbines Power* 2017; 140(4): 041510-041510-9.
11. Powell A. On the edgetone. *J Acoust Soc Am* 1961; 33: 395–409.
12. Ségoufin C, Fabre B and De Lacombe L. Experimental investigation of the flue channel geometry influence on edge-tone oscillations. *Acta Acust United Acust* 2004; 90: 966–975.
13. Fabre B and Hirschberg A. Physical modeling of flue instruments: a review of lumped models. *Acta Acust United Acust* 2000; 86: 12.
14. Castellengo M. Acoustical analysis of initial transients in flute like instruments. *Acta Acust united Acust* 1999; 85: 387–400.
15. Hosseini N, Teerling OJ, Kornilov V, et al. Thermoacoustic instabilities in a Rijke tube with heating and cooling elements. In: *Proceedings of the European combustion meeting*, Dubrovnik, Croatia, 18–21 April 2017.

16. Emmert T, Meindl M, Jaensch S, et al. Linear state space interconnect modeling of acoustic systems. *Acta Acust United Acust* 2016; 102: 824–833.
17. Chu B-T. On the generation of pressure waves at a plane flame front. *Symp Combust* 1953; 4: 603–612.
18. Lieuwen TC. *Unsteady combustor physics*. New York: Cambridge University Press, 2012.
19. Kornilov V and de Goey LPH. Combustion thermo-acoustics in context of activity and stability criteria for linear two-ports. In: *Proceedings of the European combustion meeting,* Dubrovnik, Croatia, 18–21 April 2017.
20. Raun RL, Beckstead MW, Finlinson JC, et al. A review of Rijke tubes, Rijke burners and related devices. *Prog Energy Combust Sci* 1993; 19: 313–364.